SUPPLEMENTAL EXPERIMENTAL PROCEDURES

Reagents and Drugs

The compounds in our 100 compound custom library were purchased from Sigma Aldrich (St. Louis, MO). The Sequoia and International chemical libraries were purchased from Sequoia Research Products Ltd. (Pangbourne, United Kingdom) and MicroSource Discovery Systems (Gaylordsville, CT), respectively. Annexin V-FITC and Propidium Iodide (PI) were purchased from Biovision (Moutainview, CA). Carboxydichlorofluorescein diacetate (Carboxy H_2DCF-DA) and LysoTracker Red were purchased from Invitrogen Canada (Burlington, Canada). Acridine Orange and Magic Red Cathepsin B substrate were obtained from ImmunoChemistry Technologies (Bloomington, MN). Unless otherwise noted, all other reagents were purchased from Sigma Aldrich Canada.

Cell lines

Human (OCI AML2, THP1, KG1a, NB4, OCI-M2, K562, TEX) leukemia cells were maintained in Iscove's modified Dulbecco's Medium (IMDM); HL60 and U937 cell lines, as well as the mouse MDAY-D2 line, were maintained in RPMI 1640 medium. For all cell lines except TEX, medium was supplemented with 10% fetal bovine serum (FBS), 100 μg/mL penicillin and 100 units/mL of streptomycin (all from Hyclone, Logan, UT). TEX human leukemia cells were maintained in IMDM, 15% FBS, 20 ng/mL stem cell factor (SCF), 2 ng/mL interleukin-3 (IL-3), 2 mM L-glutamine and 1%, penicillin-streptomycin. All cells were incubated at 37^{o}C in a humidified air atmosphere supplemented with 5% CO_2.

Cell growth and viability assays

Cell death was measured by staining cells with Annexin V-fluoroscein isothiocyanate (FITC) and Propidium Iodide (PI) (Biovision Research Products, Mountain View, CA) and using flow cytometry according to the manufacturer's instructions. To identify $CD34^+$ or $CD38^+$ cells, AML and normal PBSC samples were co-stained with PE–anti-CD34 (Beckman Coulter, Marseille France), and APC–anti-CD45 or Pe-Cy7-anti-CD34, Pe-Cy5-anti-CD38, APC-anti-CD45 (Becton Dickenson, San Jose CA). Cell growth and viability were assessed by the MTS assay (Promega, Madison, WI) according to the manufacturer's instructions and the sulforhodamine B assay as previously described (1, 2).

Colony formation assays

Peripheral blood samples were obtained from consenting patients with AML or normal volunteers donating G-CSF-mobilized stem cells for allotransplant. Primary cells were isolated from the blood by Histopaque-1077 (Sigma-Aldrich, St.Louis, USA) and cultured in Iscove's Modified Dulbecco's Medium (IMDM, Gibco-BRL, Gaithersburg, USA) containing 10% fetal bovine serum (FBS, Hyclone, Logan, USA) along with mefloquine or vehicle control for 48 hours. After treatment, cells were washed and plated by volume in duplicate 35 mm dishes (Nunclon, Rochester, USA) in a final volume of 1ml/dish in MethoCult GF H4434 medium (StemCell Technologies, Vancouver, Canada) and incubated at 37C, 5% CO_2 with 95% humidity. After incubation, the number of colonies containing 10 or more cells was counted on an inverted microscope as previously described (4, 5). To confirm the type of cells in the colonies, cells were picked when necessary and stained with May-Grünwald-Giemsa as described (3, 4).

Cell Differentiation Analysis

In order to assess the effect of mefloquine on leukemia cell differentiation, TEX leukemia cells were treated in culture with vehicle control, 16 mM 12-*O*-tetradecanoylphorbol-13-acetate (TPA), or 8 μM mefloquine for 48 hr. After treatment, cells were harvested, cytocentrifuged using a Shandon Elliott cytospin, fixed and stained with the DiffQuick stain set (Siemens), according to standard hematologic technique. Cells were imaged by light microscopy by the Advanced Optical Microscopy Facility, University Health Network (Toronto, ON), with an Aperio ScanScopeCS (magnification 40X). Files were analyzed with Aperio ImageScope v11.1.2.760.

Chemical screen for cytotoxic compounds

The single agent chemical screen for cytotoxic compounds was carried out as previously described (5).

Combination drug screen to identify mefloquine sensitizers

TEX leukemia cells were seeded in 96 well plates in Iscove's modified Dulbecco's medium (IMDM) containing 5% FBS, 2 mM L-glutamine, 20 ng/mL SCF, and 2 ng/mL IL-3. Cells were then treated with increasing concentrations of the drug library with and without increasing concentrations of mefloquine in triplicate. Cells were incubated at 37°C with 5% CO_2 for 72 hours. Cell growth and viability was determined using the sulforhodamine B assay.

For each combination mean excess over Bliss additivism (EOBA) values $\pm$ SD were calculated as previously described (6). EOBA values greater than two SD above the mean of the

population of drugs were considered to represent synergistic interactions drug pairs. Synergistic interactions were ranked by the degree of EOBA and the number of concentrations at which synergy was seen.

Measurement of Reactive Oxygen Species

Intracellular reactive oxygen species (ROS) were detected by staining cells with Carboxy-H_2DCFDA (final concentration 10 μM) and flow cytometric analysis as previously described. (7) . Data were analyzed with FlowJo version 8.8 (TreeStar, Ashland, OR).

Yeast Haplo-Insufficiency Profiling (HIP) Assay

To identify the primary mechanism of drug action, HIP in yeast was used to profile the fitness of ~6000 heterozygous deletion strains (8, 9) in the presence of mefloquine. The fitness assay on the deletion strains was performed as described (10) with the following modifications: 1) for barcode amplification, 0.2 μg of genomic DNA was used in a 50 μl PCR reaction containing 1 μM mix of up- or down-tag primers and 82% (v/v) of High Fidelity Platinum PCR Supermix (Invitrogen, Carlsbad, California); 2) 34 amplification cycles were used for the PCR using an extension temperature of 68° C for 2 minutes except for a final 10 minutes in the last cycle; and, 3) after 10-16 hours of hybridization, the arrays were washed in a GeneChip Fluidic Station 450 (Affymetrix, Santa Clara, CA) using the GeneFlex_Sv3_450 protocol with one additional wash cycle before the staining. The Affymetrix GeneChip Command Console Software was used to extract the intensity values from the arrays and the fitness defects were calculated for each deletion strain as log2 ratios (mean signal intensity of control/mean signal intensity of drug).

Gene-set Enrichment Analysis (GSEA) of HIP profiles

GSEA (11) was used to identify biological processes and protein complexes enriched amongst the genes associated with the greatest sensitivity to specific compounds, when individually deleted in yeast. The HIP profile of each compound (defined with a fitness defect score associated with each gene deletion) was analyzed by GSEA v2.07 in pre-rank mode (Java implementation). All default parameters were used except that the minimum and maximum gene set sizes were restricted to 5 and 300, respectively. Our gene sets were defined with Gene Ontology biological process and protein complex gene annotations obtained from the *Saccharomyces* Genome Database (http://www.yeastgenome.org) on November 12, 2011. Additional protein complex annotations based on consensus across different studies were obtained from Benschop *et. al.* 2010 (12). For each enriched gene set (FDR $\leq$ 0.01), the leading edge genes, i.e. the genes that contribute to the enrichment, were computed as in (11).

The enrichment maps in Figures 3A and S3 were generated with the Enrichment Map Plugin v1.1 (13) developed for Cytoscape (14), using the GSEA results as input. The FDR threshold was set to 0.01, and default values were used for all other parameters. For each node (i.e. enriched gene set) in each map, we computed *significance* = $-\log_{10}$(FDR) where FDR was estimated by GSEA. For nodes where *significance* equals infinity, *significance* was changed to equal 2 + the maximum non-infinite *significance* value in the given map. Node sizes were changed to be proportional to *significance*. In addition, the nodes in each map were clustered with the Markov clustering algorithm (15), using the overlap coefficient computed by the plugin as the similarity metric (coefficients less than 0.5 were set to zero) and an inflation of 2. Node colors were changed to indicate cluster membership.

Assays for Lysosome Disruption

Lysosome integrity in response to drug treatment was measured using LysoTracker and Acridine Orange staining and flow cytometry (16, 17). Briefly, cell lines or primary samples in culture were incubated with drug and then loaded with 20 μM LysoTracker or 2 μM Acridine Orange, collected, and analyzed by flow cytometry at excitation 572 nm/emission 591 nm, using the BD LSRFortessa cell analyzer flow cytometer (BD Biosciences) (LysoTracker) or the FL1 and FL3 channels, using the FACScalibur flow cytometer (BD Biosciences). Data were analyzed with FlowJo version 8.8 (TreeStar, Ashland, OR). Lysosome disruption detected using LysoTracker was measured as the percentage of cells with pale LysoTracker staining; while lysosome disruption detected with Acridine Orange was measured as the percentage of cells that lost FL3 staining.

Transmission Electron Microscopy

Cells were harvested and fixed with Graham-Karnovsky's technique as previously described (18). Next, cells were post-fixed with 1% osmium tetroxide buffered with PB for 1 h and washed again using distilled water twice for 30 minutes. Cells were then dehydrated with ethanol, washed with propylene oxide, and treated with epoxy resin, which was polymerized at 60^{o}C for 48 h. The solid epoxy blocks were sectioned on a Reichert Ultracut E microtome to 90 nm thickness, collected on 300 mesh copper grids and counterstained with uranyl acetate and lead citrate. Sections were examined with a Hitachi H7000 (Hitachi, Tokyo, Japan) transmission electron microscope at an accelerating voltage of 75 kV.

Isolation of lysosomes

Lysosomes were prepared by the methods of Matsuda and Misaka (19) with slight modifications. A minimum of 2 x 10^8 cells were taken as starting material. Cells were centrifuged at 1500 rpm for 10 min and the pellet washed with 20 ml of 0.25 M ice chilled sucrose (pH 7.4) and dissolved in 5 ml of 0.25 M sucrose containing 0.5 mM EDTA. All procedures after this step were carried out at 4 °C. Cells were lysed by using a hand homogenizer and the homogenate was centrifuged at 1020 g for 10 min. The supernatant was collected and centrifuged at 3200 g for 10 min and the pellet was discarded. This remaining supernatant was further centrifuged at 10,000 g for 35 min and pellet was dissolved in 5 ml of 0.25 M sucrose and passed through a sucrose gradient. Gradient solution was centrifuged at 3200 g for 10 min and the pellet was discarded. The supernatant was treated with 1 mM $CaCl_2$ for 15 min at 4 °C to avoid contamination with mitochondria (20) and centrifuged at 10,000 g for 40 min. The final pellet was rinsed with 0.25 M sucrose and dissolved in minimum volume of 0.25 M sucrose, stored overnight at -80 °C and was further used for lysosomal assays. Lysosomal purity was confirmed by demonstrating 5-10 fold enrichment of lysosomal acid phosphatase and cathepsin B and L activity compared to the initial homogenate, and by demonstrating enrichment of LAMP1, but not COXII, in the lysosome enriched fraction (Supplemental Figure **S3D).**

Immunoblotting

Proteins were separated on SDS-PAGE and transferred to PVDF membranes prior to antibody treatment. Blots were incubated overnight in primary antibodies raised against LAMP I (BD Transduction Laboratories), LAMP2 (Sigma-Aldrich), Actin (Cell Signaling), or COXII (Santa Cruz), as appropriate, after blocking in 5 % milk powder in PBST. Blots were further

probed using appropriate secondary antibodies conjugated with HRP and developed using Enhanced Chemiluminescence (ECL) detection (Pierce Biotechnology).

Cathepsin release from isolated lysosomes

Isolated lysosomes were treated with vehicle control, compounds, or Triton-X detergent as a positive control for 90 minutes at 37°C. After incubation, the reaction mixture was centrifuged at 15,000 g for 30 min at 4°C to pellet intact lysosomes. The activity of cathepsin released into the supernatant after lysosomal disruption was measured as described previously with some modification (21). Assays were performed in 0.1 M acetate buffer (pH 5.0) containing 250 μM Cathepsin B (Z-Arg-Arg-7-amido-4-methylcoumarin hydrochloride) or 100 μM Cathepsin L (Z-Phe-Arg-7-amido-4-methylcoumarin hydrochloride) substrates in a 96 well plate at 37 °C for 1 hr. 7-amido-4-methylcoumarin hydrochloride release was measured at 460 mm with an excitation wavelength of 380 nm.

Isolation of mitochondria

Mitochondria were purified from OCI AML2 cells using the mitochondria isolation kit (Miltenyi Biotec and as previously described (22).

Immunofluorescent Confocal Microscopy

Magic Red cathespin B substrate was used to image cathepsin B activity in control and drug-treated cell populations. Cells (2.0×10^5) were harvested after drug treatment and stained for 30 minutes at 37^oC with Magic Red cathepsin B substrate, according to manufacture's instructions (ImmunoChemistry Technologies, Bloomington, MN). After staining, cells were

transferred to microscope slides, cover-slipped, and imaged on a Zeiss LSM 700 confocal microscope (Carl Zeiss, Germany) at an objective lens magnification of 40x. Images were analyzed using LSM image analysis software (Carl Zeiss, Germany).

Knock-down of LAMP1 and LAMP2 by lentiviral shRNA

Construction of hairpin-pLKO.1 vectors (carrying a puromycin antibiotic resistance gene) containing shRNA sequences and production of short hairpin RNA viruses have been described previously in detail. The shRNAs targeting LAMP1 (Accession No. NM_005561) coding sequence are as follows: LAMP1shRNA1 5'-CCGGGAATGCAAGTTCTAGCCGGTTCTCGAGAACCGGCTAGAACTTGCATTCTTTTT-3', LAMP1shRNA2 5'-CCGGCTATCGAAATGACGGTGTTAACTCGAGTTAACACCGTCATTTCGATAGTTTTTG-3'. The shRNAs targeting LAMP2 (Accession No. NM_002294) coding sequences are as follows: LAMP2shRNA1: 5'-CCGGGTACGCTATGAAACTACAAATCTCGAGATTTGTAGTTTCATAGCGTACTTTTT-3', LAMP2shRNA2: 5'-CCGGGAAGTGAACATCAGCATGTATCTCGAGATACATGCTGATGTTCACTTCTTTTT-3'.

Lentiviral infections were performed essentially as described (23). Briefly, cells (5×10^6) in suspension culture were centrifuged and re-suspended in 10 mL media containing protamine sulfate (5 mg/mL). 3 mL of virus cocktail was added, followed by overnight incubation (37^oC, 5% CO_2) without removing the virus. The following day, cells were centrifuged, washed and fresh media with puromycin (1mg/mL) was added.

Two days later, equal numbers of live cells in each condition were plated for viability and growth assays.

In Silico Analysis of AML and LIC Gene Expression Array Datasets

The expression profile of a previously-reported lysosomal biogenesis gene signature (24) was assessed in HSCs, LICs and in the "bulk" AML tumor fraction not capable of engrafting into immune-compromised mice [(25); array dataset archived online in the NCBI Gene Expression Omnibus database, accession #: GSE30377]. In this dataset, AML patient samples were fractionated by flow cytometry into four discrete populations and analyzed in mouse bone marrow engraftment assays for presence of the LIC population. Two of four populations were determined to be LIC-positive, and two LIC-negative. Gene expression analysis was conducted on all samples (including 3 normal HSC populations), and AML samples grouped into "bulk AML" (LIC-negative) or LIC (LIC-positive) categories based on their functional phenotypes. Mean fold-change for the LIC vs. HSC, AML "bulk" tumor fraction vs. LIC, and lineage-positive vs. HSC comparisons were calculated for all lysosome biogenesis genes, and statistical significance was assessed by ANOVA. Lists of significantly differentially expressed genes were thus derived for each population comparison identified above. Visualization of gene expression profiles was accomplished using the programming package "R" (v2.13.1) (26) (http://www.R-project.org/) and the NeatMap visualization algorithm (27). Briefly, individual genes included in the visualization set were rank-ordered by sample, such that the highest-expressing sample fell in the 100^{th} percentile and the lowest expressing sample fell in the 1^{st} percentile. Genes in heatmaps were ordered by significance and fold-change, and samples were grouped by sample category. Our results were validated in independent microarray datasets

[GSE24395 for the LIC vs. HSC comparison, and GSE9476 for the bulk AML vs. normal comparison; (28, 29)] in order to confirm the significance of our findings. Raw datasets were downloaded as Affymetrix ".CEL" files where possible and analyzed and annotated as above using the "R" programming package (v2.13.1).

Quantitative Reverse Transcription-Real Time Polymerase Chain Reaction

Quantitative real-time RT-PCR was carried out as previous described (30, 31). The delta delta Ct method was used to calculate relative fold-changes in gene expression (32). Primer sequences for *LAMP1, LAMP2* and 18S rRNA are contained in Supplemental Table **S2**.

Histology studies

SCID mice were treated with mefloquine (100 mg/kg daily oral dose) or vehicle control (3 mice per treatment group) for 21 days. After sacrifice, organs were embedded with 10% buffered formalin, sectioned and stained with hematoxylin and eosin. The stained samples were scanned using Aperio Scanscope XT at 10× magnification and analyzed using Aperio ImageScope.

Lysosome Disruption in a Mouse Xenograft of AML

OCI-AML2 human leukemia cells (2.5×10^5) were injected subcutaneously into the flanks of sub-lethally irradiated (3.5 Gy) NOD/SCID mice (Ontario Cancer Institute, Toronto, ON) and mice were treated orally with vehicle control or 50 mg/kg or 100 mg/kg mefloquine daily for five days (n = 4 mice per treatment condition). After treatment, mice were sacrificed, tumors were harvested and weighed, and single cell suspensions were generated. Tumor cells

were stained with LysoTracker or Acridine Orange and analyzed by flow cytometry at excitation 572 nm/emission 591 nm, using the BD LSRFortessa cell analyzer flow cytometer (BD Biosciences) (LysoTracker) or the FL1 and FL3 channels, using the FACScalibur flow cytometer (BD Biosciences). Data were analyzed with FlowJo version 8.8 (TreeStar, Ashland, OR).

Statistical Analyses

Statistical tests were conducted, unless otherwise indicated, using GraphPad Prism v4 (GraphPad Software, La Jolla, CA) and Microsoft Excel. For statistical comparisons in cell culture assays, a two-tailed student's t-test (two-population) or one-way ANOVA (multi-population) was applied as appropriate. For statistical comparisons in data derived from animal studies or human patient samples, the Mann-Whitney test was applied for two-population comparisons and the Kruskal-Wallis test, with the Dunns post-test, was applied for three-population comparisons. Significance cut-offs of $p < 0.05$ were applied in all instances. Drug EC50s were calculated using the Median Effect method (33), with the CalcuSyn v2.0 software package (Biosoft, UK).

SUPPLEMENTAL REFERENCES

1. Kim, H.M., Han, S.B., Kim, M.S., Kang, J.S., Oh, G.T., and Hong, D.H. 1996. Efficient fixation procedure of human leukemia cells in sulforhodamine B cytotoxicity assay. *J Pharmacol Toxicol Methods* 36:163-169.
2. Skehan, P., Storeng, R., Scudiero, D., Monks, A., McMahon, J., Vistica, D., Warren, J.T., Bokesch, H., Kenney, S., and Boyd, M.R. 1990. New colorimetric cytotoxicity assay for anticancer-drug screening. *J Natl Cancer Inst* 82:1107-1112.
3. Buick, R.N., Till, J.E., and McCulloch, E.A. 1977. Colony assay for proliferative blast cells circulating in myeloblastic leukaemia. *Lancet* 1:862-863.
4. Fauser, A.A., and Messner, H.A. 1979. Identification of megakaryocytes, macrophages, and eosinophils in colonies of human bone marrow containing neurtophilic granulocytes and erythroblasts. *Blood* 53:1023-1027.
5. Sharmeen, S., Skrtic, M., Sukhai, M.A., Hurren, R., Gronda, M., Wang, X., Fonseca, S.B., Sun, H., Wood, T.E., Ward, R., et al. 2010. The antiparasitic agent ivermectin induces chloride-dependent membrane hyperpolarization and cell death in leukemia cells. *Blood* 116:3593-3603.
6. Borisy, A.A., Elliott, P.J., Hurst, N.W., Lee, M.S., Lehar, J., Price, E.R., Serbedzija, G., Zimmermann, G.R., Foley, M.A., Stockwell, B.R., et al. 2003. Systematic discovery of multicomponent therapeutics. *Proc Natl Acad Sci U S A* 100:7977-7982.
7. Pham, N.A., Jacobberger, J.W., Schimmer, A.D., Cao, P., Gronda, M., and Hedley, D.W. 2004. The dietary isothiocyanate sulforaphane targets pathways of apoptosis, cell cycle arrest, and oxidative stress in human pancreatic cancer cells and inhibits tumor growth in severe combined immunodeficient mice. *Mol Cancer Ther* 3:1239-1248.

8. Giaever, G., Flaherty, P., Kumm, J., Proctor, M., Nislow, C., Jaramillo, D.F., Chu, A.M., Jordan, M.I., Arkin, A.P., and Davis, R.W. 2004. Chemogenomic profiling: identifying the functional interactions of small molecules in yeast. *Proc Natl Acad Sci U S A* 101:793-798.

9. Smith, A.M., Heisler, L.E., St Onge, R.P., Farias-Hesson, E., Wallace, I.M., Bodeau, J., Harris, A.N., Perry, K.M., Giaever, G., Pourmand, N., et al. 2010. Highly-multiplexed barcode sequencing: an efficient method for parallel analysis of pooled samples. *Nucleic Acids Res* 38:e142.

10. Pierce, S.E., Fung, E.L., Jaramillo, D.F., Chu, A.M., Davis, R.W., Nislow, C., and Giaever, G. 2006. A unique and universal molecular barcode array. *Nat Methods* 3:601-603.

11. Subramanian, A., Tamayo, P., Mootha, V.K., Mukherjee, S., Ebert, B.L., Gillette, M.A., Paulovich, A., Pomeroy, S.L., Golub, T.R., Lander, E.S., et al. 2005. Gene set enrichment analysis: a knowledge-based approach for interpreting genome-wide expression profiles. *Proc Natl Acad Sci U S A* 102:15545-15550.

12. Benschop, J.J., Brabers, N., van Leenen, D., Bakker, L.V., van Deutekom, H.W., van Berkum, N.L., Apweiler, E., Lijnzaad, P., Holstege, F.C., and Kemmeren, P. 2010. A consensus of core protein complex compositions for Saccharomyces cerevisiae. *Mol Cell* 38:916-928.

13. Merico, D., Isserlin, R., Stueker, O., Emili, A., and Bader, G.D. 2010. Enrichment map: a network-based method for gene-set enrichment visualization and interpretation. *PLoS One* 5:e13984.

14. Smoot, M.E., Ono, K., Ruscheinski, J., Wang, P.L., and Ideker, T. 2010. Cytoscape 2.8: new features for data integration and network visualization. *Bioinformatics* 27:431-432.

15. van Dongen, S. 2000. A cluster algorithm for graphs. Amsterdam: National Research Institute for Mathematics and Computer Science in the Netherlands.

16. Broker, L.E., Huisman, C., Span, S.W., Rodriguez, J.A., Kruyt, F.A., and Giaccone, G. 2004. Cathepsin B mediates caspase-independent cell death induced by microtubule stabilizing agents in non-small cell lung cancer cells. *Cancer Res* 64:27-30.

17. Yuan, X.M., Li, W., Dalen, H., Lotem, J., Kama, R., Sachs, L., and Brunk, U.T. 2002. Lysosomal destabilization in p53-induced apoptosis. *Proc Natl Acad Sci U S A* 99:6286-6291.

18. Graham, R.C., Jr., and Karnovsky, M.J. 1966. The early stages of absorption of injected horseradish peroxidase in the proximal tubules of mouse kidney: ultrastructural cytochemistry by a new technique. *J Histochem Cytochem* 14:291-302.

19. Matsuda, K., and Misaka, E. 1974. Studies on cathepsins of rat liver lysosomes. I. Purification and multiple forms. *J Biochem* 76:639-649.

20. Yamada, H., Hayashi, H., and Natori, Y. 1984. A simple procedure for the isolation of highly purified lysosomes from normal rat liver. *J Biochem* 95:1155-1160.

21. Kawasaki, G., Mataki, S., and Mizuno, A. 1995. Ultrastructural and biochemical studies of the effect of polychlorinated biphenyl on mouse parotid gland cells. *Arch Oral Biol* 40:39-46.

22. Skrtic, M., Sriskanthadevan, S., Jhas, B., Gebbia, M., Wang, X., Wang, Z., Hurren, R., Jitkova, Y., Gronda, M., Maclean, N., et al. 2011. Inhibition of mitochondrial translation as a therapeutic strategy for human acute myeloid leukemia. *Cancer Cell* 20:674-688.

23. Xu, G.W., Ali, M., Wood, T.E., Wong, D., Maclean, N., Wang, X., Gronda, M., Skrtic, M., Li, X., Hurren, R., et al. 2010. The ubiquitin-activating enzyme E1 as a therapeutic target for the treatment of leukemia and multiple myeloma. *Blood* 115:2251-2259.

24. Sardiello, M., Palmieri, M., di Ronza, A., Medina, D.L., Valenza, M., Gennarino, V.A., Di Malta, C., Donaudy, F., Embrione, V., Polishchuk, R.S., et al. 2009. A gene network regulating lysosomal biogenesis and function. *Science* 325:473-477.

25. Eppert, K., Takenaka, K., Lechman, E.R., Waldron, L., Nilsson, B., van Galen, P., Metzeler, K.H., Poeppl, A., Ling, V., Beyene, J., et al. 2011. Stem cell gene expression programs influence clinical outcome in human leukemia. *Nat Med* 17:1086-1093.

26. 2011. *R: A language and environment for statistical computing.* Vienna, Austria: R Foundation for Statistical Computing,.

27. Rajaram, S., and Oono, Y. 2010. NeatMap--non-clustering heat map alternatives in R. *BMC Bioinformatics* 11:45.

28. Kikushige, Y., Shima, T., Takayanagi, S., Urata, S., Miyamoto, T., Iwasaki, H., Takenaka, K., Teshima, T., Tanaka, T., Inagaki, Y., et al. 2010. TIM-3 is a promising target to selectively kill acute myeloid leukemia initiating cells. *Cell Stem Cell* 7:708-717.

30. Stirewalt, D.L., Meshinchi, S., Kopecky, K.J., Fan, W., Pogosova-Agadjanyan, E.L., Engel, J.H., Cronk, M.R., Dorcy, K.S., McQuary, A.R., Hockenbery, D., et al. 2008. Identification of genes with abnormal expression changes in acute myeloid leukemia. *Genes Chromosomes Cancer* 47:8-20.

26. Schimmer, A.D., Thomas, M.P., Hurren, R., Gronda, M., Pellecchia, M., Pond, G.R., Konopleva, M., Gurfinkel, D., Mawji, I.A., Brown, E., et al. 2006. Identification of Small

Molecules that Sensitize Resistant Tumor Cells to Tumor Necrosis Factor-Family Death Receptors. *Cancer Res* 66:2367-2375.

32. Livak, K.J., and Schmittgen, T.D. 2001. Analysis of relative gene expression data using real-time quantitative PCR and the 2(-Delta Delta C(T)) Method. *Methods* 25:402-408.

33. Chou, T.C., and Talalay, P. 1984. Quantitative analysis of dose-effect relationships: the combined effects of multiple drugs or enzyme inhibitors. *Adv Enzyme Regul* 22:27-55.

Supplemental Tables

Supplemental Table S1. Patient characteristics of primary AML samples.

	Gender	Age	FAB subtype	Cytogenetic risk	Cytogenetics
Mefloquine-Sensitive					
	M	66	M4	Good	inv(16)
	F	70	M5	Intermediate	Normal
	M	65	M5	Poor	t(6;11)
	M	32	M4	Intermediate	-Y, +12q
	F	65	M5	Intermediate	Normal
	F	80	M4	Not done	Not done
	F	61	M5	Intermediate	Normal
	M	27	M3	Good	t(15;17)
	F	70	M1	Poor	del 5, 17p del, -16
Mefloquine-Insensitive					
	M	80	M4	Not done	Not done
	F	60	M4	Good	inv 16
	M	45	M6	Intermediate	normal
	M	73	M0	Intermediate	normal
	F	62	M0	Intermediate	+10
	F	61	M2	Intermediate	normal
	M	70	M1	Intermediate	normal
	F	55	M5	Intermediate	normal

Supplemental Table S2. LAMP gene PCR primers.

Gene	Strand	Sequence
LAMP1	Forward	5'- AGGCTTTCAAGGTGGAAGGT-3'
	Reverse	5'- ATGAGGACGATGAGGACCAG-3'
LAMP2	Forward	5'- ACCCCAATACAACTCACTCCA-3'
	Reverse	5'- GAAAACGGAGCCATTAACCA-3'
18S (housekeeping)	Forward	5'-AGGAATTGACGGAAGGGCAC-3'
	Reverse	5'-GGACATCTAAGGGCATCACA-3'

Attached as Microsoft Excel spreadsheets:

Supplemental Table S3. Biological processes and protein complexes associated with sensitivity to mefloquine.

Supplemental Table S4. Biological processes and protein complexes associated with sensitivity to ciclopirox olamine.

Supplemental Table S5. Biological processes and protein complexes associated with sensitivity to flubendazole.

Supplemental Table S6. Biological processes and protein complexes associated with sensitivity to clioquinol.

Supplemental Table S7. Structures of the mefloquine analogues, compounds 1-6.

R	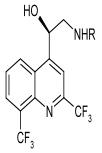 (*R*)-enantiomer	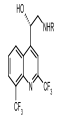 (*S*)-enantiomer
pentyl	1	2
hexyl	3	4
heptyl	5	6

SUPPLEMENTARY FIGURE LEGENDS

Supplemental Figure S1. Mefloquine induces cell death in AML cells and AML stem cells.

(A) TEX leukemia cells were treated with mefloquine (8 μM) or vehicle control. At increasing times after treatment, cells were harvested and cell viability was measured using Annexin V/PI staining and flow cytometry. Data represent the mean percent viability ± SD compared to vehicle treated controls from 3 replicates in a representative experiment.

(B) TEX leukemia cells were treated with vehicle, 16 nM TPA as a positive control for cell differentiation, or 8 μM mefloquine, for 48 hr, harvested and stained with the DiffQuick stain set, and visualized by light microscopy (40X), as outlined in the Supplemental Methods. Representative fields of view are shown; mefloquine did not induce differentiation of TEX cells in this assay.

(C) Primary AML cells were treated with increasing concentrations of mefloquine for 30 or 48 hr. After incubation, cell viability was measured by Annexin V/PI staining. Data represent the mean percent viability ± SD compared to vehicle treated controls.

(D) Primary AML samples (30 hr, n = 9; 48 hr, n = 11) and normal hematopoietic cells (30 hr, n = 5; 48 hr, n = 6) were treated with increasing concentrations of mefloquine for the times indicated. After incubation, cell viability was measured by Annexin V/PI staining and flow cytometry. Data represent the mean percent viability +/- SD from 3 replicates of a representative experiment. AML samples were divided into those that were sensitive to mefloquine (EC50 < 10 μM) and those that were insensitive to mefloquine (EC50 > 10 μM). The EC50s for these samples are reported in Figure **1E**.

(E) Primary AML cells and normal hematopoeitic cells were treated with increasing concentrations of mefloquine for 48 or 72 hours (AML: 48 hr; normal: 72 hr). The proportion of viable cells was measured by Annexin V/PI staining and flow cytometry. In addition, viability in $CD34^+/CD38^-$ (in the AML sample) and $CD34^+$ (in the normal sample) fractions was measured by anti-CD34, anti-CD38, and anti-CD45 staining, along with Annexin V/PI staining. Data represent the mean percent viability +/- SD from 3 replicates of a representative experiment.

Supplemental Figure S2. Mefloquine induces ROS production and synergizes with the artemisinin class of anti-malarials.

(A) TEX leukemia cells were treated with increasing concentrations of artesunate (upper panel) or artenimol (lower panel). 72 hours after incubation, cell viability was measured using the sulforhodamine B assay. Data represent the mean percent viability $\pm$ SD compared to the vehicle treated controls from 3 replicates in a representative experiment.

(B) Excess over Bliss additivism score heatmaps showing the effects of the combination of mefloquine with artesunate (upper panel) or artenimol (lower panel) on viability in TEX cells. Data are representative of two independent experiments.

(C) Primary AML samples (samples 1-3 mefloquine sensitive, sample 4 mefloquine insensitive) were treated with increasing concentrations of mefloquine for 48 hours. After incubation, cell viability was measured by Annexin V/PI staining and flow cytometry. Data represent the mean percent viability +/- SD from three experiments.

(D) TEX (upper panels) and OCI AML2 (lower panels) cells were treated with increasing concentrations of artesunate or artenimol for 18 hours. After incubation, ROS production was measured using 5-(and-6)-carboxy-2′7′-dichlorodihydrofluorescein diacetate (carboxy-H_2DCFDA) staining and flow cytometry. Data represent the mean fold increase in ROS production +/- SD compared to vehicle-treated control cells from three experiments. Statistically significant differences ($P < 0.05$) are as indicated.

(E) TEX cells were treated with mefloquine for 24 hours alone or in combination with the ROS scavengers α-tocopherol (3 mM) and N-acetyl-L-cysteine (NAC; 10 mM). ROS production was measured using 5-(and-6)-carboxy-2′7′-dichlorodihydrofluorescein diacetate (carboxy-H_2DCFDA) staining and flow cytometry, as outlined in the Methods

Data represent the mean ± SD fold-increase in ROS production compared to vehicle control-treated cells from 3 replicates of a representative experiment (* denotes significant inhibition of ROS production after scavenger treatment; $p < 0.05$).

Supplemental Figure S3. HIP assays of unrelated antimicrobials.

A pool of ~6000 *S. cerevisiae* heterozygote mutant strains were cultured in the presence or absence of ciclopirox olamine (**A**), flubendazole (**B**), or clioquinol (**C**) and those showing altered growth responses relative to control cells were identified. Each node represents a significantly enriched biological process/protein complex in the drug's chemogenomic profile (FDR ≤0.01, see Supplemental Experimental Procedures). The size of a node is proportional to the level of significance at which the gene category is enriched [i.e. proportional to the $-\log_{10}$ (FDR value)]. The width of an edge corresponds to the level of gene overlap between the two connected categories (i.e. gene sets). Edges are not shown where the overlap coefficient is less than 0.5. The color of a node shows the cluster membership, where clustering is based on the level of overlap between categories.

(**D**) Immunoblotting of lysosomal membrane protein LAMP I and mitochondrial protein Cytochrome c Oxidase II (COX II) in cell homogenates (H) and lysosomal enriched samples (P) from TEX and OCI AML2 cells, as indicated. The lower panel shows the Coomassie Brilliant Blue (CBB) staining of the gel.

(E) Lysosomes isolated from OCI AML2 cells were treated with 0-50 μM mefloquine for 90 minutes at 37^{o}C, followed by assessment of Cathepsin B activity. Data represent the mean Cathepsin B release ± SD (AU = arbitrary units), in excess of the vehicle-treated control, for mefloquine treated samples, as indicated.

Supplemental Figure S4. Mefloquine disrupts lysosomes.

(A) TEX cells were treated with or without 10 μM mefloquine for 24 hours, fixed, and imaged by transmission electron microscopy as described in the methods. Representative images taken at 30,000x magnification are shown. Lysosomes are indicated by black arrows; Scale bar: 500 nm.

(B) OCI AML2 cells were treated with vehicle control or 10 μM mefloquine for 24 hours and stained with LysoTracker or Acridine Orange. LysoTracker or Acridine Orange uptake was quantified by flow cytometry. Results represent the % lysosomal integrity compared to vehicle treated controls and are reported as the mean +/- SD of 3 replicates of a representative experiment. Statistically significant differences ($P < 0.05$) between treatments are as indicated.

(C) TEX cells were treated with vehicle control, 8 or 10 μM mefloquine for 24 hours and stained with Acridine Orange or LysoTracker. Uptake of the dyes was quantified by flow cytometry. Results represent the % lysosomal integrity compared to vehicle treated controls and are reported as mean +/- SD of 3 replicates of a representative experiment. Statistically significant differences ($P < 0.05$) between treatments are as indicated.

(D) THP1 cells were treated with vehicle control, 8 or 10 μM mefloquine for 24 hours and stained with LysoTracker. Uptake was quantified by flow cytometry. Results represent the % lysosomal integrity compared to vehicle treated controls and are reported as mean +/- SD of 3 replicates of a representative experiment.

(E) Left panel: TEX cells were treated with 10 μM mefloquine or vehicle control for 6 hours, fixed, and imaged by transmission electron microscopy as outlined in the methods. Images were taken at 10,000x and 30,000x magnification. NIH ImageJ software was

used to visualize and score intact lysosomes. Data are represented as mean percent intact lysosomes ± SD. Right panel: TEX cells were treated with mefloquine (5 and 10 μM,) for 24 hours and ROS production measured using 5-(and-6)-carboxy-2′7′-dichlorodihydrofluorescein diacetate (carboxy-H_2DCFDA) staining and flow cytometry. Data represent the mean fold increase in ROS production +/- SD compared to vehicle-treated control cells from 3 replicates of a representative experiment.

(F) Dose-response relationship in TEX cells treated with tigecycline (0-24 μM, 72 hr exposure).

(G) TEX cells were treated with vehicle control, 10 μM mefloquine, or 2.5-7.5 μM tigecycline for 24 hours and stained with Acridine Orange. After staining, Acridine Orange uptake was quantified by flow cytometry. Data represent the % lysosomal integrity compared to vehicle-treated controls +/- SD from 3 replicates of a representative experiment.

(H) Dose-response relationship in TEX and OCI AML2 cells treated with ivermectin (0-20 μM, 48 hr exposure).

(I) TEX and OCI AML2 cells were treated with vehicle control, or 2.5-10 μM ivermectin for 24 hours and stained with LysoTracker. After staining, LysoTracker uptake was quantified by flow cytometry. Data represent the mean % lysosomal integrity compared to vehicle-treated controls +/- SD from 3 replicates of a representative experiment.

(J) Dose-response relationship in TEX and OCI AML2 cells treated with ciclopirox olamine (0-5 μM, 48 hr exposure).

(K) TEX and OCI AML2 cells were treated with vehicle control, or 0.3125-5 μM ciclopirox olamine for 24 hours and stained with LysoTracker. After staining, LysoTracker uptake

was quantified by flow cytometry. Data represent the mean % lysosomal integrity compared to vehicle-treated controls +/- SD from 3 replicates of a representative experiment.

(L) TEX cells were treated with mefloquine (0 or 10 μM) for 24 hours alone or in combination with the ROS scavenger α-tocopherol (3 mM), and lysosome disruption was measured using LysoTracker (left panel) and Acridine Orange (right panel) and flow cytometry. Data represent the % lysosomal integrity compared to vehicle treated controls +/- SD compared to vehicle-treated control cells from 3 replicates of a representative experiment.

(M) TEX cells were treated with 8 μM mefloquine alone, or with the pan-caspase inhibitor ZVAD-FMK (100 μM), for 48 hours. After treatment, cell viability was measured by Annexin V/PI staining and flow cytometry. Data represent the mean percent viability relative to vehicle treated controls $\pm$ SD from 3 replicates of a representative experiment.

(N) K562 cells were treated with vehicle 0-10 μM mefloquine, with or without 100 μM Pepstatin A co-treatment, for 24 hours and cell viability measured by Annexin V/PI and flow cytometry. Data represent the mean % viability compared to vehicle-treated controls +/- SD from 3 replicates of a representative experiment

Supplemental Figure S5. Characterization of mefloquine analogues' effects on cell viability and lysosome integrity.

(A) OCI AML2 cells were treated with increasing concentrations of (+/-)-erythro-mefloquine racemic mixture for 48 hr. After incubation, cell viability was measured by MTS. Relative viability was calculated in comparison to the vehicle-treated controls. Data represent the mean percent viability +/- SD from 3 replicates of a representative experiment.

(B) OCI AML2 cells were treated with increasing concentrations of (+/-)-threo-mefloquine racemic mixture for 48 hr. After incubation, cell viability was measured by MTS. Relative viability was calculated in comparison to the vehicle-treated controls. Data represent the mean percent viability +/- SD from 3 replicates of a representative experiment.

(C) OCI AML2 cells were treated with increasing concentrations of the indicated mefloquine analogue for 48 hr. After incubation, cell viability was measured by MTS. Relative viability was calculated in comparison to the vehicle-treated controls. Data represent the mean percent viability +/- SD from 3 replicates of a representative experiment.

(D) OCI AML2 cells were treated with increasing concentrations of the indicated mefloquine analogue for 24 hr. After incubation, lysosome integrity was measured by LysoTracker staining and flow cytometry. Relative lysosome integrity was calculated in comparison to the vehicle-treated controls. Data represent the mean percent lysosome integrity +/- SD from 3 replicates of a representative experiment.

Supplemental Figure S6. Effects of shRNA-mediated LAMP1 knockdown on mefloquine-sensitive TEX cells.

(A) Quantitative real-time RT-PCR analysis of lentiviral shRNA-mediated knockdown of LAMP1 in TEX cells. Data represent the mean $\pm$ SD change in LAMP1 mRNA expression compared to the TEX untransduced controls (* denotes significant knock-down of LAMP1 gene expression, compared to the control shRNA; $p < 0.05$).

(B) Protein expression of LAMP1 after shRNA-mediated knockdown in individual clones by immunoblotting; actin was used as a loading control. Molecular weights of proteins (in kDa) are indicated.

(C) TEX cells were infected with shRNA targeting LAMP1 or control sequences. The total number of viable cell was measured by trypan blue 6 days after infection. Data are presented as cell counts (x 10^6), and represent the mean +/- SD of four replicates in a representative experiment. (* denotes significant decrease of growth and viability, compared to the control shRNA; $p < 0.05$).

(D) Lysosome integrity of control and LAMP1-shRNA transduced TEX cells was measured by Acridine Orange staining and flow cytometry. Relative lysosome integrity was calculated in comparison to the control shRNA-transduced cells. Data represent the mean percent lysosome integrity +/- SD from 3 replicates of a representative experiment. (* denotes significant decrease of lysosome integrity, compared to the control shRNA; $p < 0.05$).

Supplemental Figure S7. Effects of shRNA-mediated LAMP1 knockdown on mefloquine-resistant THP1 cells.

(A) Quantitative real-time RT-PCR analysis of lentiviral shRNA-mediated knockdown of LAMP1 in THP1 cells. Data represent the mean $\pm$ SD change in LAMP1 mRNA expression compared to the THP1 untransduced controls (* denotes significant knock-down of LAMP1 gene expression, compared to the control shRNA; $p < 0.05$).

(B) Protein expression of LAMP1 after shRNA-mediated knockdown in individual clones by immunoblotting; actin was used as a loading control. Molecular weights of proteins (in kDa) are indicated.

(C) THP1 cells were infected with shRNA targeting LAMP1 or control sequences. The total number of viable cell was measured by trypan blue staining over time. Data are presented as cell counts (x 10^6), and represent the mean +/- SD of four replicates in a representative experiment.

(D) Lysosome integrity of control and LAMP1-shRNA transduced THP1 cells was measured by Acridine Orange staining and flow cytometry. Relative lysosome integrity was calculated in comparison to the control shRNA-transduced cells. Data represent the mean percent lysosome integrity +/- SD from 3 replicates of a representative experiment. (* denotes significant decrease of lysosome integrity, compared to the control shRNA; $p < 0.05$).

(E) Dose-response relationship in THP1 cells treated with LeuLeuOMe (0-100 μM, 48 hr exposure).

(F) THP1 cells were treated with vehicle control, or 25-100 μM LeuLeuOMe for 24 hours and stained with LysoTracker. After staining, LysoTracker uptake was quantified by flow

cytometry. Data represent the mean % lysosomal integrity compared to vehicle-treated controls +/- SD from 3 replicates of a representative experiment (* $p < 0.05$).

Supplemental Figure S8. Effects of shRNA-mediated LAMP1 knockdown on mefloquine-resistant U937 cells.

(A) Quantitative real-time RT-PCR analysis of lentiviral shRNA-mediated knockdown of LAMP1 in U937 cells. Data represent the mean ± SD change in LAMP1 mRNA expression compared to the U937 untransduced controls (* denotes significant knock-down of LAMP1 gene expression, compared to the control shRNA; $p < 0.05$).

(B) Protein expression of LAMP1 after shRNA-mediated knockdown in individual clones by immunoblotting; actin was used as a loading control. Molecular weights of proteins (in kDa) are indicated.

(C) U937 cells were infected with shRNA targeting LAMP1 or control sequences. The total number of viable cell was measured by trypan blue staining over time. Data are presented as cell counts (x 10^6), and represent the mean +/- SD of four replicates in a representative experiment.

(D) Lysosome integrity of control and LAMP1-shRNA transduced U937 cells was measured by Acridine Orange staining and flow cytometry. Relative lysosome integrity was calculated in comparison to the control shRNA-transduced cells. Data represent the mean percent lysosome integrity +/- SD from 3 replicates of a representative experiment. (* denotes significant decrease of lysosome integrity, compared to the control shRNA; $p < 0.05$).

(E) Dose-response relationship in U937 cells treated with LeuLeuOMe (0-100 μM, 48 hr exposure).

(F) U937 cells were treated with vehicle control, or 25-100 μM LeuLeuOMe for 24 hours and stained with LysoTracker. After staining, LysoTracker uptake was quantified by flow

cytometry. Data represent the mean % lysosomal integrity compared to vehicle-treated controls +/- SD from 3 replicates of a representative experiment (* $p < 0.05$).

Supplemental Figure S9. Lysosome disruption as a therapeutic strategy in AML.

(A) OCI AML2 cells were treated with increasing concentrations of LeuLeuOMe for 24 hours. After treatment, ROS production was measured using 5-(and-6)-carboxy-2′7′-dichlorodihydrofluorescein diacetate (carboxy-H_2DCFDA) staining and flow cytometry. Data represent the mean fold increase in ROS production +/- SD compared to vehicle-treated control cells from 3 replicates of a representative experiment.

(B) Lysosomes isolated from OCI AML2 cells were treated with mefloquine (20 μM), artesunate (10 μM), artenimol (10 μM), or LeuLeuOMe (100 μM) for 90 min at 37 °C. Cathepsin B release into the supernatant was measured as described in the Supplemental Experimental Procedures. Data represent the mean Cathepsin B release ± SD over the baseline untreated controls from three replicates within a representative experiment (AU = arbitrary units). Significant elevations in Cathepsin B activity after treatment were evident (* $p < 0.05$; ** $p < 0.01$; *** $p < 0.001$).

Supplemental Figure S10. Cathepsins and a lysosome biogenesis gene expression signature are up-regulated in AML.

(A) Normal CD34+ hematopoietic cells and primary AML patient cells were fixed and imaged by transmission electron microscopy as described in the methods. Representative images taken at 30,000x magnification are shown. Lysosomes are indicated by black arrows. N = nucleus; m = mitochondrion. Scale bar: 500 nm.

(B) Ordered heat maps illustrating the over-expression of distinct subsets of lysosome biogenesis genes in the LIC compartment (n = 12 samples) compared to HSC (n = 5); data are derived from the publicly accessible dataset GSE24395, archived on the Gene Expression Omnibus. Genes are rank-ordered by fold-change and significance.

(C) Ordered heat maps illustrating lysosomal cathepsin gene expression in LIC (n = 12 samples) and HSC (n = 5); data are derived from the publicly accessible dataset GSE24395, archived on the Gene Expression Omnibus. Genes are rank-ordered by fold-change and significance.

(D) Scatter plots demonstrating the over-expression of lysosomal cathepsin mRNA in primary AML samples compared to normal CD34+ bone marrow cells. Statistically significant differences between the two populations were assessed using the Mann-Whitney test; statistically significant differences ($P < 0.05$) between population groups are as indicated. Data are derived from the publicly accessible dataset GSE9476, archived on the Gene Expression Omnibus.

Supplemental Figure S11. Toxicity of mefloquine treatment.

Hematoxalin and eosin stained sections of mouse liver, kidney and heart from one representative control and one representative mefloquine-treated mouse.

Supplemental Figure S12. Effects of 100 mg/kg/day oral mefloquine on mouse body weight.

Measurement of mouse body weight in vehicle-treated and mefloquine-treated mice (100 mg/kg x 21 days); n = 7 per treatment condition.